Langmuir

Article

pubs.acs.org/Langmuir

The Colloidal State of Tannins Impacts the Nature of Their Interaction with Proteins: The Case of Salivary Proline-Rich Protein/Procyanidins Binding

Olivier Cala,[†,‡] Erick J. Dufourc,[‡] Eric Fouquet,[†] Claude Manigand,[‡] Michel Laguerre,[‡] and Isabelle Pianet*[,†]

[†]Univ. Bordeaux and CNRS, Institut des Sciences Moléculaires, UMR 5255, CESAMO, 351 cours de la Libération, Talence F-33405, France

[‡]Univ. Bordeaux and CNRS, Institute of Chemistry & Biology of Membranes & Nanoobjects, CBMN, UMR 5248, F-33600 Pessac, France

Supporting Information

ABSTRACT: While the definition of tannins has been historically associated with its propensity to bind proteins in a nonspecific way, it is now admitted that specific interaction also occurs. The case of the astringency perception is a good example to illustrate this phenomenon: astringency is commonly described as a tactile sensation induced by the precipitation of a complex composed of proline-rich proteins present in the human saliva and tannins present in beverages such as tea or red wines. In the present work, the interactions between a human saliva protein segment and three different procyanidins (B1, B3, and C2) were investigated at the atomic level by NMR and molecular dynamics. The data provided evidence for (i) an increase in affinity compared to shortest human saliva peptides, which is accounted for by protein "wraping around" the tannin, (ii) a specificity in the interaction below tannin critical micelle concentration (CMC) of ca. 10 mM, with an affinity scale such that C2 > B1 > B3, and (iii) a nonspecific binding above tannin CMC that conducts irremediably to the precipitation of the tannins/protein complex. Such physicochemical findings describe in accurate terms saliva protein−tannin interactions and provide support for a more subtle description by oenologists of wine astringency perception in the mouth.

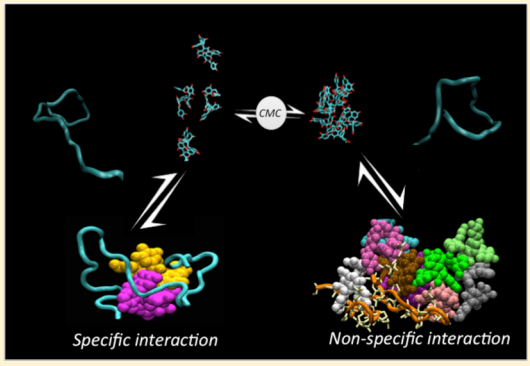

INTRODUCTION

Tannins have long been described to complex and precipitate proteins, cellulose, pectin, or even alkaloids in a nonspecific way.[1] Since the work of Haslam[2] and Hagerman and Butler,[3] there are pieces of evidence indicating that specific interaction takes place, that can explain part of their potential health benefits which are not exclusively due to their antioxidant activity.[4,5] Thus, interaction specificity appears as the key player of the use of these phytochemicals as drugs. In this paper, we show how the specificity of tannins/proteins interaction can be ensured by the control of the colloidal state of the tannins through an example: how the astringency of wine can be perceived. Tannins are commonly described to elicit the extremely complex "in mouth" perception of astringency, a sensation which can be described in oenology by not less than 33 words grouped in 7 different terms.[6] Even if a consensus of opinion suggests that this tactile sensation is the consequence of a recognition process between human salivary proteins, mainly proline-rich proteins (PRPs) and tannins,[7,8] the precipitation of the PRP−tannins complex formed, and the consequent loss of lubrication in oral saliva cannot explain in itself the diversity of the vocabulary used to describe astringency, terms which can be associated to qualities or default, especially in red wines. Beyond the physiological (especially the salivary protein composition[9]) and psychological factors[10] that mediate its perception, new physicochemical quantities (binding constants, stoichiometry and atomic structure of complexes, driving forces for association, etc.) will provide solid grounds for a better understanding of the multifaceted sensation of astringency.

In a recent study, we demonstrated that procyanidins (tannins belonging to the flavan-3-ol family, Figure 1) exhibit different affinities for a proline-rich peptide of 14-residues length representative of a proline-rich repeat domain of human salivary PRPs, depending on their conformational preference and degree of polymerization.[11] Notably, we have shown that procyanidins preferentially adopting an extended conformation such as B2[12] or C2[13] were able to play a role of bidentate ligand, hence binding two peptides and initiating the formation of a complex tannins−peptides network susceptible to

Received: October 5, 2012
Revised: November 15, 2012
Published: November 21, 2012

   dx.doi.org/10.1021/la303964m | *Langmuir* 2012, 28, 17410−17418

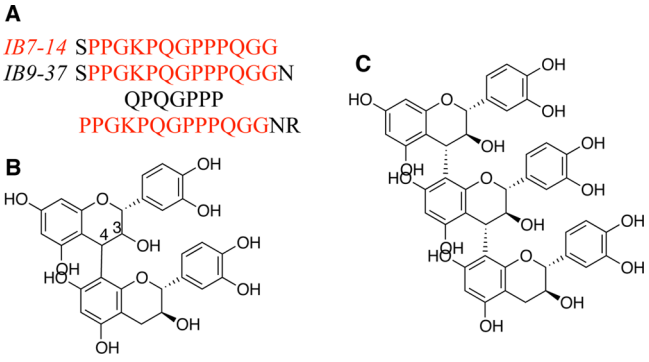

Figure 1. (A) Amino acid sequences of IB7−14 and IB9−37 aligned to show repeated domains. (B) Chemical structures of procyanidin B1 (3*R*,4*S*) and B3 (3*S*,4*R*), and (C) procyanidin C2.

precipitation. In this work, we also evidence the role played by the tannins colloidal state[15] to direct specific versus nonspecific interactions.

The choice of a shorter peptide represented a necessary step to understand at an atomistic level the different steps that govern the recognition process between human salivary PRPs and tannins. It was also required to gain structural understanding of this class of proteins which combine many, if not all, difficulties for obtaining detailed structural analysis: PRPs indeed belong to the natively unfolded proteins family so that X-ray cannot be applied, leading NMR spectroscopy as the sole method of investigation.[14,16] However, the high degeneracy in the primary sequence of these proteins, where three amino acids account for 70−80% of the total residues (approximately 40% proline, 21% glycine, and 17% glutamine residues), the presence of repeated domains (3 to 5, depending on the PRPs considered[17]), and the absence of any stable tertiary structure preclude conventional NMR assignment strategies, so that the assignment of shortest peptides is a necessary prerequisite.

In the present study, we choose to work on a longest PRP peptide (IB9−37, Figure 1, 60% of the full length human IB9). Our aim was (i) to assign all its proton chemical shifts, despite spectral overcrowding, and allow to map interactions with tannins; (ii) to gain valuable insight about its conformational preferences; (iii) and to understand the discrepancies observed between tannin affinities measured with shortest peptides (K_d commonly in the millimolar range[18,19]) and full-length PRPs (K_d in the micromolar range[20−22]). The explanation proposed 15 years ago by Charlton et al.[20] was that the increased length of the protein allows it to fold and "wrap around" the tannin, a mechanism also proposed recently to explain the ion mobility spectra differences between the naked PRP IB5 and the complex formed when epigallocatechin gallate is added to the protein mixture.[23]

To investigate all these aspects, we used as a saliva protein model IB9−37 and as wine tannins three different procyanidins (the dimers B1 and B3 and the trimer C2, Figure 1) that have been found recently to show very different binding constants toward a smaller saliva protein fragment, IB7−14. Two techniques were combined for gaining insight into the interaction mode at an atomistic level: NMR and molecular dynamics.

EXPERIMENTAL SECTION

Peptide Synthesis and Purification. Amino acids, solid-phase support, HOBt, and HBTU for solid-phase synthesis were purchased from Novabiochem (Läufelfingen, Switzerland). The synthesis of $IB9_{37}$ (Figure 1) was performed on an Applied Biosystem peptide synthesizer 433A (PE Biosystem, Courtaboeuf, France) using the Fmoc strategy according to a previously described method.[24] The peptide was purified by HPLC (Water 2487 dual wavelength absorbance detector) using a Nova Pak C18 column (Alliance chromatographic system, Waters, Saint-Quentin-en-Yvelines, France) and was controlled by MALDI mass spectrometry as described earlier.[24]

Procyanidin Dimers and Trimer Synthesis. The procyanidins dimers B1, B3 and trimer C2 (Figure 1) were synthesized and purified as previously described.[25]

Circular Dichroism. CD spectra were recorded on a JASCO J-815 spectrometer. The peptide sample was prepared in a H_2O/ethanol mixture 88:12 at pH 3.5 and 298 K. Measurements were conducted on a peptide concentration range between 0.2 and 1 mM. The spectra were recorded over a 190−270 nm range in 0.1 mm cells, and the curves were deconvoluted using the homemade CD-friend program developed by Buchoux[26] with poly(L-proline) and poly(L-lysine) spectra recorded in the same conditions as standard curves for pure type II helix and unstructured states, respectively.

NMR Experiments. For the peptide 3D structure, regular 1D and 2D spectra were recorded on a BrukerAvance III 700 and 800 MHz instrument equipped with a 5 mm diameter BBI Gradient probe or a TCI HCND z-gradient 5 mm Cryprobe. In all experiments, water suppression was achieved with a watergate sequence.[27] For titration experiments, 1D proton, TOCSY, and DOSY spectra were recorded for all tannin concentrations.

Peptide, 0.5 mM, was dissolved in a mixture composed of 5 mM deuterated acetic acid, 70% H_2O, 18% D_2O, and 12% deuterated ethanol. The pH was adjusted to 3.5 in order to mimic usual acidity in wine.

A ^1H spectral width of 7700 Hz was used for all the experiments. For structural purpose, TOCSY and NOESY spectra were recorded using 512 increments, and 32 scans (acquisition time: 10h). For titration purposes, TOCSY spectra were recorded using 256 increments and 16 scans (acquisition time 2h). A contact time value of 100 ms was used for TOCSY experiments and of 120 ms for NOESY experiments. $^1H-^{13}C$ HSQC or HMBC experiments were acquired using 512 increments and 32 or 64 scans for a total acquisition time of 7 and 14h, respectively.

Diffusion NMR Experiments. Diffusion ordered spectroscopy (DOSY) NMR was used to measure translational diffusion coefficients, *D*. It allows differentiation of species related to their effective molecular weight, size, and shape, leading very different applications from intermolecular interaction[28−30] to molecular aggregation processes[15,31] or ionic liquids.[32] Diffusion measurements were performed using ^1H NMR bipolar pulsed gradients.[33,34] The following parameters were used: spectral width, 12 ppm; scan number, 128; recycling delay, 2 s; intergradient delay Δ, 150 ms; gradient pulse duration δ, 2 ms. The pulse gradients (G) were incremented from 2 to 95% of the maximum gradient strength in a linear ramp in 16 steps. The diffusion coefficient, D can be obtained by fitting a specific resonance area, I, obtained at different gradient powers (G) using eq 1:

$$I/I_0 = \exp[-\gamma^2 G^2 D\delta^2(\Delta - \delta/3)] \quad (1)$$

where I_0 is the signal intensity for $G = 0$.

NMR Data Analysis. For titration experiments, selected proton chemical shift variations were analyzed using eq 2:[35]

$$\Delta\delta_{obs} = \frac{1}{2}\Delta\delta_{max}(1 + K_d/n[P_i] + [T_i]/n[P_i]) - \{(1 + K_d/n[P_i] + [T_i]/n[P_i])^2 - 4[T_i]/n[P_i]\}^{1/2} \quad (2)$$

where $\Delta\delta_{obs}$ is the chemical shift variation (ppm) upon tannin binding, $\Delta\delta_{max}$ is the chemical shift difference between the chemical shift of the protein free and saturated with tannins, K_d is the dissociation constant expressed in M, $[T_i]$ is the total concentration of polyphenols able to bind the peptide (in M) by taking into account their self-association

dx.doi.org/10.1021/la303964m | *Langmuir* 2012, 28, 17410−17418

(K_a of the self-association process has been evaluated to be 6.5 M^{-1} for B3, 7.0 M^{-1} for B1, and 5.0 M^{-1} for C2,[15]), $[P_0]$ is the total concentration of peptide (in M), and n is the number of polyphenol binding sites. K_d, n, and $\Delta\delta_{max}$ were calculated using a least-squares-fitting routine within the software program Microsoft EXCEL. Above a specific concentration of tannins (the tannin CMC, commonly above 8−12 mM), nonspecific binding occurs and was fitted with a linear regression. The same approach was used with measured diffusion coefficients, D, that were inserted into eq 2 instead of chemical shifts, δ.

Molecular Dynamics. *A. Peptide Alone.* Molecular modeling calculations were performed according to a previously published procedure[18] on a Linux workstation running MacroModel version 6.5 (Schrodinger Inc.). Conformational minima were found using the modified AMBER* (1991 parameters) force field as implemented and completed in the MacroModel program. Built structures were minimized to a final RMSD gradient of 0.005 kJ·Å^{-1}·mol^{-1} via the truncated Newton conjugate gradient (TNCG) method (1000 cycles). Calculations were performed with the GB/SA continuum solvation model.[36] The solvent chosen was water. In all cases, the extended cutoff option was used throughout (VdW = 8 Å, electrostatic = 20 Å, and H-bond = 4 Å). It must be mentioned that tannins are very simple molecules from a chemical point of view, and hence, the corresponding parameters in actual force fields are well-defined and of high quality. Stochastic dynamic simulations were accomplished using the variant of molecular dynamics that is implemented in MacroModel. The chosen temperature was 1000 K, the time step was 1 fs, the total simulation time in each case was 10 ns, and 200 snapshots were saved for each run. All saved conformers were fully minimized and ranked by ascending energy (TNCG, 1000 steps). Minimization and molecular dynamics runs were performed under constraints coming from NOESY experiments. The following distance constraints were chosen according to the NOE correlation intensities: strong, 2.2 ± 0.4 Å; medium, 3.5 ± 0.9 Å; and weak, 5.0 ± 0.5 Å. These distance constraints are chosen in order to ensure three contiguous classes of distances without overlap but also without any "forbidden" intervals.

B. Interaction of IB9$_{37}$ with the C2 Trimer. Calculations were accomplished using GROMACS version 4.5 and the GROMOS96 force field (G43a1). The C2 molecule was parametrized using the Dundee PRODRG2 server Web site version 2.5 (beta) (http://davapc1.bioch.dundee.ac.uk/prodrg/). The protein and nine molecules of C2 were set in a SPC (simple point charge) cubic water box with dimensions: 100 × 100 × 100 Å^3 containing around 99 170 atoms. Protein was simply neutralized, and no salts were added. Protein was located in the center of the box, and the nine C2s were regularly led in the box in order to completely surround the protein. Molecular dynamics runs were performed at constant temperature (300 K, time constant for coupling τ_p = 0.1 ps) and pressure (P = 1 bar, τ_p = 0.5 ps) with a Berendsen coupling. Time step = 2 fs, PME (particle meshed Ewald) method was on with a cubic grid (1 Å), VdW cutoff = 10 Å, and frames were saved every 1000 steps. The tannin and protein concentrations are equivalent to 15.7 and 1.7 mM, respectively.

C. Calculation of Amphiphilic Surfaces. Molecular lipophilicity potentials (MLP) were calculated at the atomic level with a homemade program[18] originating from an idea of Audry et al.[37] and using an exponential function.[38] The fragmental atomic constants used were those of Broto et al.,[39] and MLP maps were calculated via the MLP program.[40]

RESULTS

3D Structure of IB9−37. The peptide synthesis and purification has been performed using the strategy already described previously for this kind of peptide.[24] Purity has been controlled using MALDI-TOF spectrometry. Only one peak at 3580.81 Da (monoisotopic mass corresponding to M+H) was observed in the spectrum. The global yield of this synthesis reached 23%, corresponding to an amino acid grafting level up to 96%. The 3D structure of IB9−37 was determined in a winelike medium (water/ethanol, 88:12, pH 3.5) using three different methods: circular dichroism, NMR, and molecular modeling.

The IB9−37 CD spectrum was submitted to a spectral deconvolution using a linear combination of random, α helix, β sheet, and helix II CD standard curves as described in the Experimental Section (Supporting Information Figure S1). The best fit was obtained with a combination of 40% type II helix and 60% random coil, as previously reported for the IB7−14[18] or even for the whole IB7 peptide,[24] with the proportion of PII helix being directly related to the proportion of Proline residues in the peptide sequence (16 prolines for 39 residues, i.e., 41%).

The whole proton assignment and the subsequent sequential attribution of IB9−37 were achieved in spite of severe signal overlap. That was possible because of the good superimposition between its TOCSY/NOESY spectrum and those of the IB7−14 peptide (Figure 2). Indeed, limited chemical-shift dispersion and the proton NMR signal pattern homology with a shorter peptide are elements which confirm undoubtedly the unfolded nature of the protein.[16,41] The IB7−14 peptide amino acid sequence is repeated twice in the IB9−37 peptide: the 14 N-

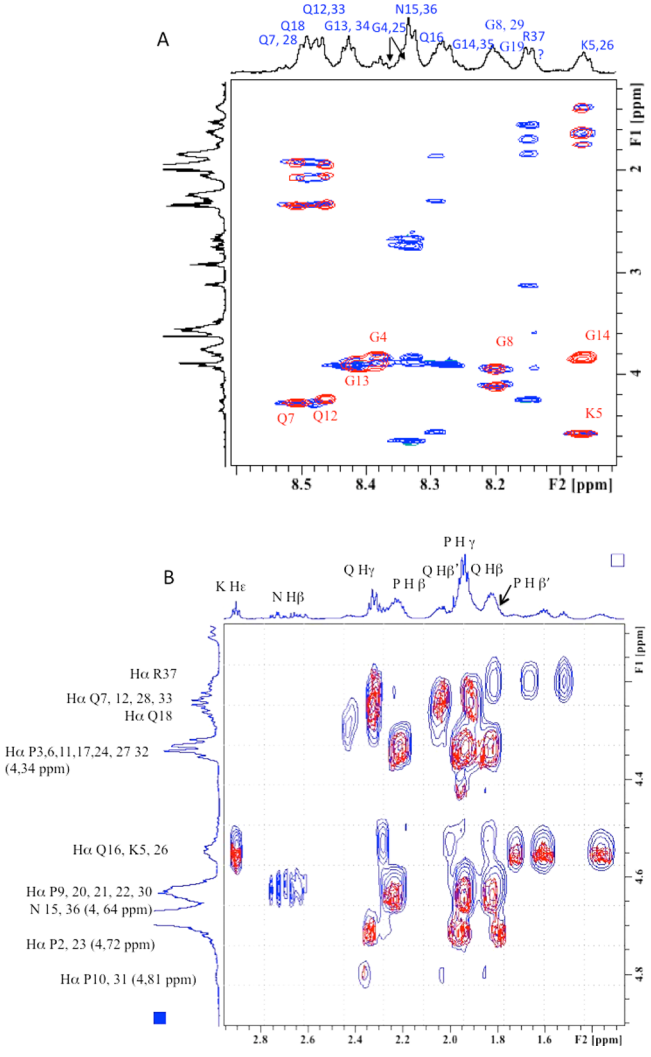

Figure 2. Protons assignment of IB9−37 (in blue) compared with those of IB7−14 (in red); data taken from a previous study.[18] TOCSY spectrum: (A) NH region and (B) proline region.

dx.doi.org/10.1021/la303964m | Langmuir 2012, 28, 17410−17418

terminal and the 23−36 parts (Figure 1). Concerning the assignment of all the NH protons (figure 2a), only the NH resonance of G14 is shifted and is explained by the fact that this residue is not any more the C-terminal amino acid of the IB9−37 peptide. However, the chemical shifts of its two alpha protons remain unchanged (3.82; 3.86 ppm). The resonance signal observed at 8.14 ppm is most probably related to a glycine NH resonance of a minor peptide conformer as was already observed on the TOCSY spectrum of IB7−14 (a conformer with cis-proline as previously suggested by Pascal et al. for the IB5 peptide[42]).

The same phenomenon is observed in the prolines region: four different proline Hα chemical shifts are observed (Figure 2b). A first group observed at 4.345 ppm and corresponding to the isolated prolines P6, P17, P27 or at the end of a proline sequence (P3, P11, P24, P32).[43] A second group with Hα chemical shift detected at 4.64 ppm is assigned to prolines surrounded by prolines (P9, P20, P21, P22, P30). A third group whose Hα resonates at 4.72 ppm can be undoubtedly assigned to P2 thanks to NOE correlations observed with the Hα and β of serine 1, and probably corresponds also to P23, and a fourth resonance detected at 4.81 ppm has been assigned to P10 and P31. The total resolution of this spectral region was achieved by dissolving the peptide in D_2O in order to decrease the residual signal of water and avoid water suppression that saturates the neighbor resonances belonging to Hα prolines. Some resonances, that were not present in the IB7−14 spectra, were easily assigned to residues N15 and N36 (NH: 8.396) or R37 (NH: 8.326). Two signal fingerprints, belonging to glutamine residues, are observed at NH chemical shifts of 8.388 and 8.407. These glutamines were, respectively, assigned to Q16 and Q18 thanks to (i, i + 1) NOEs observed with N15 and P17, respectively. Results are compiled in Supporting Information Table S1.

The sequential assignment was achieved through NOESY spectra where 12 (i, i + 1) NOEs were listed in the NH-Hα region, 14 in the NH-Hβ,γ region, and 4 in the CHα and Pδ region. The proton chemical shift values, the poor NOE response, and the J(NH−CHα) values confirm the predominance of random coil in the peptide organization.[44]

Minimization and molecular dynamics runs were performed under the NOEs and ^3J(CHα-NH) coupling constraints. At the end of the calculation process, 10 3D structures were selected. A rapid glance at these structures allows observing that an extended conformation predominates due to the presence of a high level of Proline residues that confers a type II organization helix when a series of at least 3 consecutive Prolines are present. The other part of the peptide is organized in random coil (Figure 3). The Ramanchandran plot (Supporting Information Figure S2) confirms these results, and shows that some residues belong to the type II helix region.

Titration Experiments. Procyanidins B1, B3, and C2 were added progressively to a 0.5 mM peptide solution to reach a final concentration of 20 mM in tannins. Tannins−peptide interaction was monitored by following chemical shift and peptide diffusion variations all along the titration experiments. Significant chemical shift variations were observed on G13/G34, G14/G35, K5/K26 NH, and P9/P20/P30 Hα. The solution remained clear below a tannin concentration close to 10−12 mM, whatever the tannin used (dimers B1, B3 or trimer C2). Above this concentration, the solution became cloudy and a precipitate appeared at higher concentrations of tannins. Concomitantly, all the NH proton resonances were shifted to higher field (Figure 4). The chemical shift variations observed all along the titration experiments exhibits two distinct phases

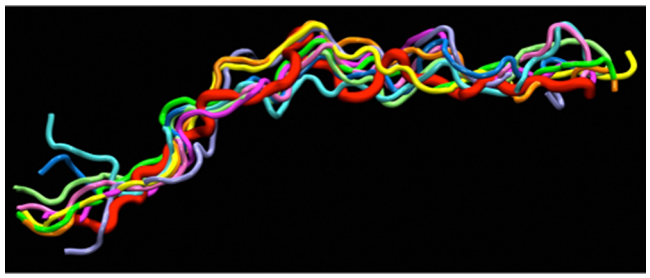

Figure 3. Ten best conformations of IB9−37 obtained from molecular dynamics under NMR constrains (see text). The red bold trace represents the lowest energy conformation.

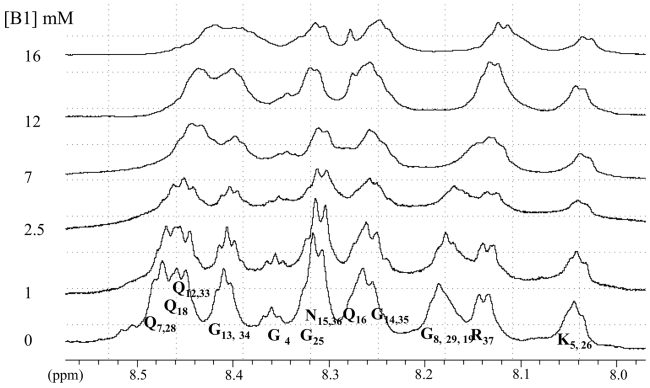

Figure 4. Chemical shift variations of peptide IB9−37 upon B1 addition. NH region.

(Figure 5A). The first phase, which takes place below a tannin concentration of 10 mM, can be fitted using eq 2 and give the dissociation constant K_d and the number of binding sites n for each tannin (Table 1). A second phase appears when the tannins concentration is higher than 10 mM. In this case, the chemical shifts evolve linearly at each tannin addition. This phenomenon can be accounted for by nonspecific interaction occurring when tannins preferentially exist as aggregated forms, which is confirmed by diffusion experiments (vide infra).

Using DOSY NMR, it is possible to follow the evolution of the translational diffusion coefficient of the peptide (D) that can be used in this case as a probe to follow the evolution of its size during the titration (Figure 5B). The same phenomenon is observed as for the chemical shift changes, and a break in the curve evolution is also observed for tannins concentration above 10 mM: below this concentration, D evolves until a plateau corresponding to a maximal diffusion difference of 0.4 × 10^{-10} m^2/s for the trimer and 0.15 × 10^{-10} m^2/s for the two dimers (the starting value is 2.4 × 10^{-10} m^2/s for the peptide alone). For tannin concentrations above 10 mM, D values decrease significantly and linearly as the tannin concentration increases. This phenomenon confirms what was previously expected by molecular dynamics calculations for the IB7−14 peptide[11] and observed by NMR and fluorescence for interaction experiments performed on procyanidin B3 and trypsin:[45] two distinct processes occur depending on the aggregation state of tannins. Below their CMC (10−15 mM[15]), a specific interaction takes place between the tannin and the

dx.doi.org/10.1021/la303964m | Langmuir 2012, 28, 17410−17418

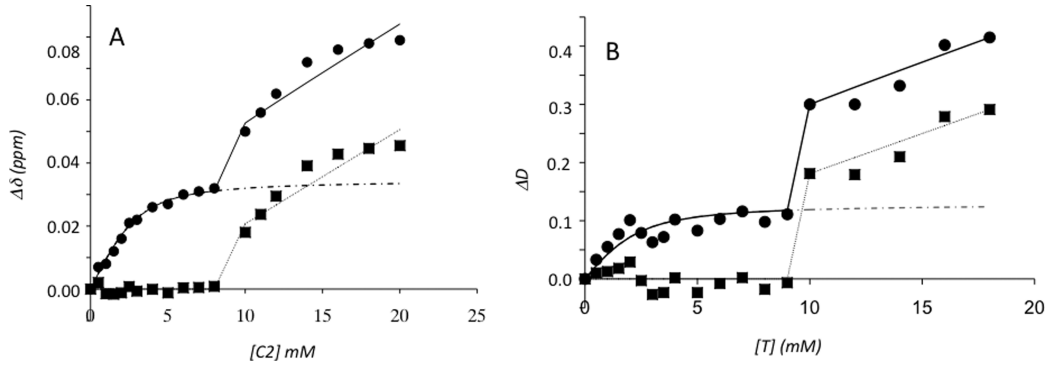

Figure 5. (A) Comparison of the observed (symbols) and fitted chemical shifts differences of the Hα of P9, P20, P30 with increasing C2 concentrations. Peptide concentration was 0.5 mM, and tannins were added to obtain the final concentration indicated on the *x*-axis. Fitting parameters were as follows: Below 10 mM, experimental points were fitted with eq 2; K_d, 0.5 mM; $\Delta\delta_{max}$, 0.034; *n*, 2.7; and RMS = 1.75×10^{-5}. Above 10 mM, a linear curve ($y = 0.00299x - 0.00092$) was added to eq 2 in order to take into account non specific binding. Nonspecific binding (···■···) is obtained from the difference between experimental (●) and specific binding (- - -). (B) Comparison of the observed (symbols) and fitted diffusion coefficient differences of peptide with increasing B1 concentrations. Peptide concentration was 0.5 mM, and tannins were added to obtain the final concentration indicated on the *x*-axis. Fitting parameters were as follows: Below 10 mM, experimental points were fitted with eq 2; K_d, 1 mM; ΔD_{max}, 0.015; *n*, 2.5; and RMS = 3.68×10^{-4}. Above 10 mM, a linear curve ($y = 0.0133x - 0.0348$) was added to eq 2 in order to take into account nonspecific binding. Non specific binding (···■···) is obtained from the difference between experimental (●) and specific binding (- - -).

Table 1. Binding Data[a]

	IB9−37			IB7−14[b]		
tannins	K_d (mM)	ΔD_{max}	*n*	K_d (mM)	ΔD_{max}	*n*
B3	1.4 ± 0.5	0.05	2.4 ± 0.6	8.0 ± 0.9	0.7	3.0 ± 0.5
B1	0.9 ± 0.2	0.1	2.6 ± 0.4	2.9 ± 1.4	0.4	3.0 ± 0.4
C2	0.4 ± 0.1	0.4	2.4 ± 0.7	0.4 ± 0.1	1.6	3.0 ± 0.2

[a]Dissociation constant (K_d) and number of tannins binding sites (*n*) were obtained from the fit of experimental chemical shifts of K5, G13, G14, G34, and G35 NH, as well as P2 and P6 Hβ using eq 2. The different K_d and *n* values obtained were averaged and are reported as means ± SD. [b]From Cala et al.[11]

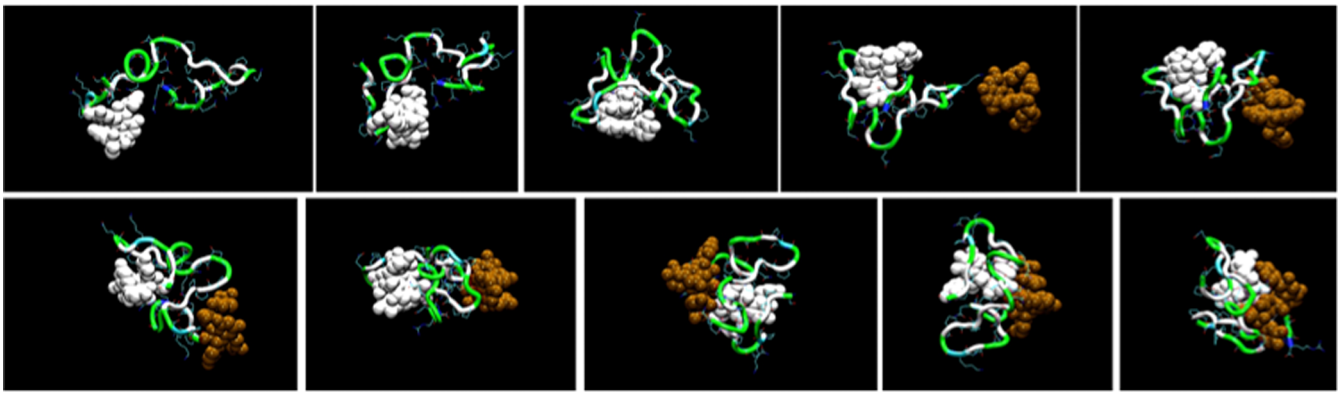

Figure 6. Snapshots centered on the C2 (white and brown) peptide (green rubban) complex selected during the molecular dynamics run (total of 66 ns).

peptide, whereas above the CMC nonspecific interactions dominate.

Equation 2 is used to fit experimental points (chemical shifts or diffusion coefficients variations) obtained for tannin concentrations below 10 mM and to determine the physicochemical parameters governing the interaction process. Table 1 reports the dissociation constants, K_d, and the number of binding sites, *n*, obtained for the three studied tannins.

The analysis of K_d values demonstrates that the same affinity scale is observed for the procyanidins than previously observed for IB7−14, that is to say C2 > B1 > B3. However, it is noteworthy that, especially for B1 and B3, K_d values are significantly lower than those for the shorter IB7−14 peptide (Table 1 also reports values obtained for IB7−14[11,46]). A similar result has been already described by Charlton et al.[20] who demonstrated that the affinity toward different tannins of the full-length IB5 peptide was significantly stronger than that with a shorter peptide containing only one proline-rich repeat unit.[47] The most likely explanation they proposed was that the increased length of the peptide allowed folding and "wrapping around" the tannin. This hypothesis can be reinforced by the number of binding sites found for IB9−37 compared to IB7−14: *n* slightly decreases in the longer peptide (Table 1), suggesting that proline-rich proteins cannot act as a "tannin sponge" whenever the tannin concentration is kept under the CMC.

dx.doi.org/10.1021/la303964m | *Langmuir* 2012, 28, 17410−17418

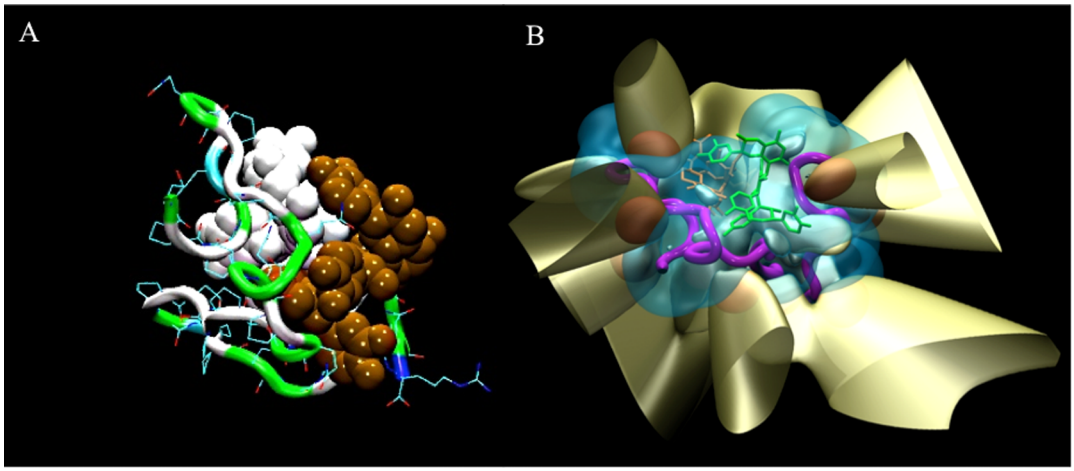

Figure 7. 3D structure of a complex composed of a IB9−37 (A, green trace; B, magenta trace) and two C2 trimers (A, white and brown; B, green and orange) after completion of a 66 ns all atoms molecular dynamics run (A) and its molecular lipophobicity profile (B): hydrophilic potential is in blue, lipophobic in red (not seen here because in the back of the image), and the interface in beige.

Above the procyanidin CMC (currently above 10 mM), experimental points start a linear progression that can be fitted. Such a phenomenon can be explained by nonspecific binding occurring between a tannin aggregate with more than one protein leading to precipitation of the peptide-tannin complex as previously proposed in ref 11.

Binding Sites. As evidenced by titration experiments, IB9−37 has been shown to fix specifically two to three procyanidin dimers or trimers (Table 1). The higher chemical shift variations are observed for the NH protons, in general (they all shift to high field frequencies), and in particular for glycines G4/G25, G8/G29, G13/G34. Some variations to low field frequencies are also observed for the Hα and Hβ resonances of prolines P2/P23, P3, P6, P11... and P9, P20, P21, P22.

Another way to determine the number of tannins bound to the peptide and their location is to use molecular dynamics calculation. For this purpose, we placed at random in a water box of 100 Å side, one peptide in its preferred conformation (Figure 3) and nine procyanidin trimers C2 in their major conformation.[13] These in silico conditions correspond to a ratio [T]/[P] of 9, with a C2 concentration of 15 mM, that is, close to its CMC.[15] Figure 6 presents some snapshots selected all along the molecular dynamics run. It is noteworthy that the binding of one (at t = 1.3 ns) and then two (t = 7.7 ns) C2 induces a notable change in the peptide conformation. From a fibrillar and flexible conformation, the peptide appears to wrap around the two C2 trimers, rendering impossible the binding of more tannins. At t = 66 ns, a reorganization of the two tannins, which stack together, occurs probably to stabilize the complex. During that time, the other tannins self-associate to form a small aggregate composed of up to seven procyanidins C2 (see Supporting Information Figure S3).

Unfortunately, NMR was not able to give information neither about the tannins location onto the peptide nor about changes in the peptide conformation. NOESY experiments were performed on a solution containing 0.5 mM peptide and 1 mM B1, which is largely below the tannin CMC. In these conditions, no significant NOE cross-peaks were observed between the tannins and the peptide and no supplementary intramolecular NOE cross-peak was observable for the peptide. This suggests that the complex as seen by molecular dynamics is probably dynamic with respect to the NMR time scale (milli- to microseconds).

DISCUSSION

A molecular description of the interaction between tannins and saliva proline-rich proteins, which are thought to be responsible for astringency, can be reached step by step, thanks to more than 30 years of research accomplished by numerous teams in the world. The model currently accepted was proposed by Jöbstl et al.[48] in 2004 in which three stages were described: (i) the simultaneous binding of the multidentate polyphenols to several sites on the free protein whose structure evolves from a loose and extended conformation to a more compact one; (ii) as the polyphenol concentration rises, polyphenols cross-link different protein molecules leading to dimerization; and (iii) aggregation into larger particles that finally precipitate.

In a previous work[11] as well as in the present work, we try to provide our contribution to improve this model by looking at both the peptide and the procyanidin behaviors. The proline-rich peptide IB9−37, which adopts an extended and flexible conformation when free of any interaction, changes its conformation when it interacts with procyanidins. It surrounds up to three procyanidins when its length is sufficient. Such a behavior was postulated by Charlton et al.[20] to explain the gain in affinity with respect to shortest peptides. In a recent study, Canon et al.[23] used ion mobility spectrometry to explore the conformation change of the IB5 proline-rich peptide when interacting with the epigallocatechin gallate tannin and interpreted their data by a transition from an extended to a more compact structure as the number of tannins bound to the protein increased. The present work confirms the first stage of the recognition process between a PRP and tannin in which a structural rearrangement of the peptide occurs as shown by molecular dynamics experiments. Three more elements confirm the hypothesis of a rearrangement process in which the peptide surrounds the tannins: (i) the gain in affinity by a factor 3−5 compared to the shortest peptide IB7−14; (ii) IB9−37 is not able to fix more than three procyanidins dimers or trimers in a specific way just like IB7−14 despite the presence of two peptide repeats units instead of 1 for IB7−14; (iii) the 3D structure preference that adopts tannins is not involved in the precipitation mechanism as observed for the shortest peptide

dx.doi.org/10.1021/la303964m | Langmuir 2012, 28, 17410−17418

IB7−14.[11] However, the different procyanidins tested present an affinity order equivalent to that measured on IB7−14 (C2 > B1 > B3).

The binding sites, related to specific association, are located in the same hydrophilic domains involving proline residues as seen on the end MD run snapshot, Figure 7A. This is especially seen when calculating the molecular lipophobicity profile as shown in Figure 7B. This calculation allows representing the various hydrophilic, hydrophobic, and interfacial regions in a particular molecular complex.[18] In our case, the hydrophilic region is on one side of the complex and tannins are binding the protein from this hydrophilic side. However, it was difficult to get precise information from NMR spectra due to resonances overlapping and absence of any intermolecular NOE, possibly related to on/off exchange of tannins between binding sites and solution. Concerning the initiation of a PRP-tannin network that leads to precipitation, our work clearly demonstrates that it is influenced by the colloidal state of the tannin itself.[15] Above he tannins CMC (around 10 mM for procyanidin dimers or trimers), nonspecific interactions dominate as shown in the titration experiments and pellets appear in the solution. It has been shown previously on the shortest peptide IB7−14 that aggregates composed of about 10 procyanidin molecules first attach the peptide as a whole in the specific hydrophilic sites of the peptide and thereafter develop interactions at random with the lipohilic part of the peptide. In this case, when aggregated, procyanidins can bridge two or more different peptides leading to the formation of a network that further precipitates.[11] This phenomenon has been also observed for trypsin that precipitates as the procyanidin B3 concentration rises.[45]

In conclusion, our work can help to improve the currently proposed model of tannins−protein interaction for which the interaction can conduct or not to the complex precipitation depending on the colloidal state of the tannin. This is tentatively sketched in Figure 8 where the route to soluble or insoluble complexes is represented and depends on the initial tannin colloidal state.

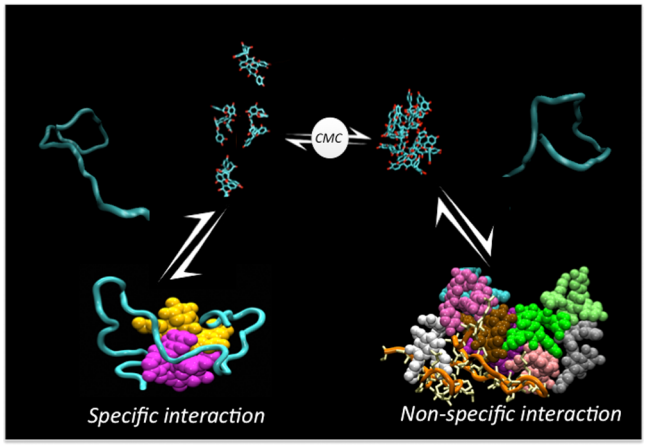

Figure 8. Proposed binding model that depends on the colloidal state of the tannin. Below the CMC, specific interactions occur between a flexible an extended PRP. The interaction generates a conformational change of the protein, that surrounds the tannin. Above tannin the CMC, nonspecific interactions dominate, leading to the complex precipitation.

■ ASSOCIATED CONTENT

Supporting Information

Additional table and figures as described in the text. This material is available free of charge via the Internet at http://pubs.acs.org.

■ AUTHOR INFORMATION

Corresponding Author

*E-mail: i.pianet@ism.u-bordeaux1.fr.

Notes

The authors declare no competing financial interest.

■ ACKNOWLEDGMENTS

The Conseil Interprofessionnel du Vin de Bordeaux (CIVB, 1, Cours du XXX juillet, F-33075 Bordeaux Cedex) is deeply acknowledged for financial support. The Aquitaine Government is thanked for supporting equipment set up in the CESAMO, IECB, and TGIR NMR Platforms. Financial support from the TGE RMN THC FR 3050 for conducting the research is gratefully acknowledged. Axelle Grélard (CBMN) and Cécile Courrèges (IECB) are deeply acknowledged for setting up the NMR equipment of IECB, Noël Pinaud and Jean Michel Lasnier (CESAMO, ISM) for the NMR equipment of CESAMO, and Christelle Absalon, Claire Mouche, and Christianne Vitry (CESAMO, ISM) for the mass spectrometer equipment of CESAMO. Funding from Conseil Interprofessionnel du Vin de Bordeaux (CIVB, 1, Cours du XXX juillet, F-33075 Bordeaux Cedex), Aquitaine Government, and TGE RMN THC FR 3050 is acknowledged.

■ ABBREVIATIONS

B1: epicatechin (4β-8) catechin
B3: catechin (4α-8) catechin
C2: catechin (4α-8) catechin (4α-8) catechin
CD: circular dichroism
CMC: critical micellar concentration
DOSY: diffusion ordered spectroscopy
HBTU: *O*-benzotriazole-*N*,*N*,*N*′,*N*′- tetramethyl-uronium-hexafluorophosphate
HOBt: *N*-hydroxybenzotrizole
K_d: dissociation constant
n: number of binding sites
PRP: proline-rich protein

■ REFERENCES

(1) Bate-Smith, E. C. Astringency in foods. *Foods* **1954**, *23*, 124.
(2) Haslam, E. Polyphenol-protein Interaction. *Biochem. J.* **1974**, *139*, 285−288.
(3) Hagerman, A. E.; Butler, L. G. The specificity of proanthocyanidin-protein interactions. *J. Biol. Chem.* **1981**, *256*, 4494−4497.
(4) Stevenson, D. E.; Hurst, R. D. Polyphenolic phytochemicals- just antioxidants or much more? *Cell. Mol. Life Sci.* **2007**, *64*, 2900−2916.
(5) Chung, K. T.; Wong, T. Y.; Wei, C. I.; Huang, Y. W.; Lin, Y. Tannins and human health: a review. *Crit. Rev. Food Sci. Nutr.* **1998**, *38*, 421−464.
(6) Gawel, R.; Oberholster, A.; Leigh Francis, I. A "mouth-feel Wheel": terminology for communicating the mouth-feel characteristics of red wine. *Aust. J. Grape Wine Res.* **2000**, *4*, 74−95.
(7) Bajec, M. R.; Pickering, G. J. Astringency: Mechanisms and Perception. *Crit. Rev. Food Sci. Nutr.* **2008**, *48*, 858−875.
(8) McRae, J. M.; Kennedy, J. A. Wine and Grape Tannin Interactions with Salivary Proteins and their impact on astringency: A review of current research. *Molecules* **2011**, *16*, 2348−2364.

(9) Lu, Y.; Bennick, A. () Interaction of tannin with human salivary proline-rich proteins. *Arch. Oral Biochem.* **1998**, *43*, 717−728.
(10) Martens, M. A philosophy for sensory science. *Food Qual. Preference* **1999**, *10*, 233−244.
(11) Cala, O.; Pinaud, N.; Simon, C.; Fouquet, E.; Laguerre, M.; Dufourc, E. J.; Pianet, I. NMR and molecular modeling of wine tannins binding to saliva proteins: revisiting astringency from molecular and colloidal prospects. *FASEB J.* **2010**, *24*, 4281−4290.
(12) Tarascou, I.; Barathieu, K.; Simon, C.; Ducasse, M. A.; Andre, Y.; Fouquet, E.; Dufourc, E. J.; de Freitas, V.; Laguerre, M.; Pianet, I. A 3D structural and conformational study of procyanidin dimers in water and hydro-alcoholic media as viewed by NMR and molecular modeling. *Magn. Reson. Chem.* **2006**, *44*, 868−880.
(13) Tarascou, I.; Ducasse, M. A.; Dufourc, E. J.; Moskau, D.; Fouquet, E.; Laguerre, M.; Pianet, I. Structural and conformational analysis of two native procyanidin trimers. *Magn. Reson. Chem.* **2007**, *45*, 157−166.
(14) Neri, D.; Billeter, M.; Wider, G.; Wutrich, K. NMR determination of residual structure in a urea-denatured protein, the 434-repressor. *Science* **1992**, *257*, 1559−1563.
(15) Pianet, I.; Andre, Y.; Ducasse, M. A.; Tarascou, I.; Lartigue, J. C.; Pinaud, N.; Fouquet, E.; Dufourc, E. J.; Laguerre, M. Modeling procyanidin self-association processes and understanding their micellar organization: A study by diffusion NMR and molecular mechanics. *Langmuir* **2008**, *24*, 11027−11035.
(16) Smet, C.; Leroy, A.; Sillen, A.; Wieruszeski, J.-M.; Landrieu, I.; Lippens, G. Accepting its random coil nature allows a partial NMR assignment of the neuronal tau protein. *ChemBioChem* **2004**, *5*, 1639−1646.
(17) Kauffman, D. L.; Keller, P. J.; Bennick, A.; Blum, M. Alignment of amino-acid and DNA sequences of human proline-rich proteins. *Crit. Rev. Oral Biol. Med.* **1993**, *4*, 2287−2292.
(18) Simon, C.; Barathieu, K.; Laguerre, M.; Schmitter, J. M.; Fouquet, E.; Pianet, I.; Dufourc, E. J. Three-Dimensional Structure and Dynamics of Wine Tannin-Saliva Protein Complexes. A Multitechnique Approach. *Biochemistry* **2003**, *42*, 10385−10395.
(19) Baxter, N. J.; Lilley, T. H.; Haslam, E.; Williamson, M. P. Multiple interaction between polyphenols and a salivary proline-rich protein repeat result in complexation and precipitation. *Biochemistry* **1997**, *36*, 5566−5577.
(20) Charlton, A. J.; Baxter, N. J.; Lilley, T. H.; Haslam, E.; McDonald, C. J.; Williamson, M. P. Tannin interactions with a full-length human salivary proline-rich protein display a stronger affinity than with single proline-rich repeats. *FEBS Lett.* **1996**, *382*, 289−292.
(21) Carvalho, E.; Mateus, N.; Plet, B.; Pianet, I.; Dufourc, E. J.; De Freitas, V. Influence of wine pectic polysaccharides on the interactions between condensed tannins and salivary proteins. *J. Agric. Food Chem.* **2006**, *54*, 8936−8944.
(22) McRae, J. M.; Falconer, R. J.; Kennedy, J. A. Thermodynamics of grape and wine tannin interaction with polyproline: Implications for red wine astringency. *J. Agric. Food Chem.* **2010**, *58*, 12510−12518.
(23) Canon, F.; Ballivian, R.; Chirot, F.; Antoine, R.; Sarni-Manchado, P.; Lemoine, J.; Dugourd, P. Folding of a salivary Intrinsically Disordered Protein upon binding to tannins. *J. Am. Chem. Soc.* **2011**, *133*, 7847−7852.
(24) Simon, C.; Pianet, I.; Dufourc, E. J. Synthesis and CD study of the human salivary Proline-Rich Protein: IB7. *J. Pept. Sci.* **2002**, *9*, 125−131.
(25) Tarascou, I.; Barathieu, K.; Andre, Y.; Pianet, I.; Dufourc, E. J.; Fouquet, E. An improved synthesis of procyanidin dimers: Regio- and stereocontrol of the interflavan bond. *Eur. J. Org. Chem.* **2006**, 5367−5377.
(26) Buchoux, S. Vers un nouveau modèle de déstabilisation des membranes biologiques par lipopetides. Thesis in Chemistry, University of Bordeaux, 2008, p 177.
(27) Piotto, M.; Saudek, V.; Sklenar, V. Gradient-tailored excitation for single-quantum NMR spectroscopy of aqueous solutions. *J. Biomol. NMR* **1992**, *22*, 661−666.
(28) Cohen, Y.; Avram, L.; Frish, L. Diffusion NMR Spectroscopy in Supramolecular and Combinatorial Chemistry: An old parameter-New insights. *Angew. Chem., Int. Ed.* **2005**, *44*, 520−554.
(29) Boisselier, E.; Ornelas, C.; Pianet, I.; Ruiz, J.; Astruc, D. Four generations of water soluble dendrimers with 9 to 243 benzoate T ethers: synthesis and dendritic effects on their ion paring with Acetyl choline, Benzyltriethylammonium and dopamine in water. *Chem.—Eur. J.* **2008**, *14*, 5577−5587.
(30) Ornelas, C.; Boisselier, E.; Martinez, V.; Pianet, I.; Aranzaes, J. R.; Astruc, D. New water-soluble polyanionic dendrimers and binding to acetylcholine in water by means of contact ion-pairing interactions. *Chem. Commun.* **2007**, 5093−5095.
(31) Carteau, D.; Pianet, I.; Brunerie, P.; Guillemat, B.; Bassani, D. M. Probing the initial events in the spontaneous emulsification of trans-anethole using dynamic NMR spectroscopy. *Langmuir* **2007**, *23*, 3561−3565.
(32) Duluard, S.; Grondin, J.; Bruneel, J.-L.; Pianet, I.; Grélard, A.; Campet, G.; Delville, M.-H.; Lassègues, J.-C. Lithium solvation and diffusion in the 1-butyl-3-methylimidazolium bis-(trifluoromethanesulfonyl)imid ionic liquid. *J. Raman Spectrosc.* **2008**, *39*, 627−632.
(33) Stejskal, E. O.; Tanner, J. E. Spin diffusion Measurements: Spin echoes in the presence of a time dependent field gradient. *J. Chem. Phys.* **1965**, *42*, 288−292.
(34) Wu, D.; Chen, A.; Johnson, C. S. Flow Imaging by Means of 1D Pulsed-Field-Gradient NMR with Application to Electroosmotic Flow. *J. Magn. Reson., Ser. A* **1995**, *115*, 123−126.
(35) Charlton, A. J.; Baxter, N. J.; Khan, M. L.; Moir, A. J. G.; Haslam, E.; Davies, A. P.; Williamson, M. P. Polyphenol/peptide Binding Precipitation. *J. Agric. Food Chem.* **2002**, *50*, 1593−1601.
(36) Still, W.; Tempezyck, A.; Hawley, R. C.; Hendrickson, T. Semianalytical treatment of solvation for molecular mechanics and dynamics. *J. Am. Chem. Soc.* **1990**, *112*, 6127.
(37) Audry, E.; Dubost, J. P.; Dallet, P.; Langmois, M. H.; Colleter, J. C. Le potentiel de lipophilie moléculaire: application à une série d'amines β-adrénolytiques. *Eur. J. Med. Chem.* **1986**, *24*, 155−161.
(38) Fauchére, J. L.; Quarendon, P.; Kaetterer, L. Estimating and representing hydrophobicity potential. *J. Mol. Graphics* **1988**, *6*, 203−206.
(39) Moreau, G.; Broto, P.; Fortin, M.; Turpin, C. Réalisation sur ordinateur d'un screening de structures moléculaires de substances potentiellement anxiolytiques à l'aide de la technique d'autocorrélation. *Eur. J. Med. Chem.* **1988**, *23*, 275−281.
(40) Laguerre, M.; Saux, M.; Dubost, J. P.; Carpy, A. A program for the calculations of molecular lipophilicity potential in proteins. *Pharm. Sci.* **1997**, *3*, 217−222.
(41) Mukrasch, M. D.; von Bergen, M.; Biernat, J.; Fischer, D.; Griesinger, C.; Mandelkow, E.; Zwecstetter, M. The "jaws" of the Tau-Microtubule Interaction. *J. Biol. Chem.* **2006**, *282*, 12230−12239.
(42) Pascal, C.; Paté, F.; Cheynier, V.; Delsuc, M. A. Study of the interactions between a Proline-Rich Protein and a Flavan-3-ol by NMR: Residual Structures in the natively unfolded Protein provides anchorage points for the ligands. *Biopolymers* **2009**, *91*, 745−756.
(43) Wishart, D.; Bigam, C. G.; Holm, A.; Hodges, R. S.; Sykes, B. D. 1H, 13C and 15N random coil chemical shifts of the common amino acids. I. Investigations of nearest-neighbor effects. *J. Biomol. NMR* **1995**, *5*, 67−81.
(44) Schwarzinger, S.; Kroon, G. J. A.; Foss, T. R.; Chung, J.; Wright, P. E.; Dyson, H. J. Sequence-Dependent correction of random coil chemical shifts. *J. Am. Chem. Soc.* **2001**, *123*, 2970−2978.
(45) Gonçalves, R.; Mateus, N.; Pianet, I.; Laguerre, M.; de Freitas, V. Mechanisms of tannin-induced trypsin inhibition: A molecular approach. *Langmuir* **2011**, *27*, 13122−13129.
(46) Cala, O.; Fabre, S.; Dufourc, E. J.; Fouquet, E.; Pianet, I. NMR of human saliva protein/wine tannin complexes. Towards deciphering astringency with physico-chemical tools. *C. R. Chim.* **2010**, *13*, 449−452.
(47) Murray, N. J.; Williamson, M. P.; Lilley, T. H.; Haslam, E. Study of the interaction between salivary proline-rich proteins and a

polyphenol by 1H-NMR spectroscopy. *Eur. J. Biochem.* **1994**, *219*, 923−935.
(48) Jöbstl, E.; O'Connell, J.; Fairclough, J. P.; Willamson, M. P. Molecular model for astringency produced by polyphenol/protein interactions. *Biomacromolecules* **2004**, *5*, 942−949.